UNDERSTANDING PHOTOMETRIC PHASE ANGLE CORRECTIONS

John Africano[(1)], Paul Kervin[(3)], Doyle Hall[(1)],
Paul Sydney[(2)], John Ross[(2)],
Tamara Payne[(2)], Steve Gregory[(2)],
Kira Jorgensen[(4)], Kandy Jarvis[(4)], Tracy Parr-Thumm[(4)],
Gene Stansbery[(5)], and Ed Barker[(5)]

[(1)]Boeing LTS, Inc., 1250 Academy Park Loop Suite 110, Colorado Springs, CO, 80910, USA,
Email: john.l.africano@boeing.com
[(2)]Boeing LTS, Inc., 535 Lipoa Parkway, Kihei, Maui, HI, 96753, USA
[(3)]AFRL Detachment 15, 535 Lipoa Parkway, Kihei, Maui, HI, 96753, USA
[(4)]ESC Group, PO Box 58447, Mail Code JE104, Houston, TX, 77258, USA, Email: kira.abercromby1@jsc.nasa.gov, kandy.s.jarvis1@jsc.nasa.gov, tracy.l.thumm1@jsc.nasa.gov
[(5)]NASA Johnson Space Center, 2101 NASA Parkway, Mail Code KX, Houston, TX, 77058, USA,
Email: eugene.g.stansbery@nasa.gov, edwin.s.barker@nasa.gov

ABSTRACT

Determining the actual physical dimensions of resident space objects (RSO) from radar cross section (RCS) measurements or optical signatures has proven to be problematic. For radar, RCS is a complex function of size, shape, material, and wavelength of the radar. NASA developed the empirically derived size estimation model (SEM) to statistically relate RCS to physical size for small debris. The SEM is not appropriate for individual objects and especially intact objects. Converting optical brightness to actual object size for both known and unknown objects is a real challenge for the optical debris community. Optical signatures are complex functions of the shape, type, albedo and scattering functions of the object's surfaces. In general surface reflectance does not behave solely as combinations of specular or Lambertian surfaces. Adding to these complexities is the fact that the objects change orientation during the observing periods due to the real or apparent rotation of the object. For uniformity, observers participating in the IADC optical debris campaigns have agreed to reduce their data using the diffuse Lambertian spherical phase function correction to 0° phase angle. A size for the RSO is then determined after the phase correction is made. It is also well understood that rocket bodies, spacecraft, debris, and most manmade objects have complex irregular shapes. These complex irregular shapes and even simple shapes produce time varying amounts of shadowing which complicate the interpretation of the photometric signatures and the resulting size estimations. This paper will address some of the limitations in using the diffuse Lambertian spherical phase angle correction.

1. INTRODUCTION

NASA has been observing the space debris population in low Earth orbit (LEO) for more than a decade using radars. The size distribution of debris objects is extremely important for understanding the risk of collision between orbiting objects, as well as the effect of those collisions on active payloads. Operational spacecraft are struck routinely by microscopic man-made and natural objects, usually with little or no significant damage. However, as the size of those objects increases, the potential for serious damage increases dramatically.

One way to estimate the size of an object is to use the radar cross section (RCS). The RCS of an object is a complex function of size, shape, and material composition of the object, and the wavelength of the illuminating radar. It is also a function of the orientation of the object with respect to the radar site. NASA has developed the empirically-derived Size Estimation Model (SEM) (Bohannon and Young, 1993) to statistically relate RCS to physical size for small debris, using the concept of an equivalent sphere diameter (ESD). The SEM is not intended to determine the size for individual objects, particularly for intact payloads. Using the SEM, the range in ESD size for a single object can vary by as much as a factor of 10 or more, depending on the particulars of the radar observations.

Information on the size distribution of objects in deep space, however, is still incomplete. For this region of space, optical telescopes are the sensors of choice. Since the mid 1990s, both NASA and the European Space Agency (ESA) have been developing optical debris survey techniques. Converting optical brightness to object size for resident space objects (RSO) has proven to be equally as challenging for the optical community as converting RCS is for the radar community. Optical brightness is a complex function of the shape, size, surface material composition, albedo, and scattering functions of the object's surfaces, as well

as the solar illumination conditions. Similar to radar, the brightness is also a function of the orientation of the object not only with respect to the observing station, but also with respect to the illumination source, usually the Sun. Note that this orientation usually will change during an observation or during the observing campaign.

For uniformity, observers participating in the Inter-Agency Space Debris Coordination Committee (IADC) optical debris campaigns have agreed to reduce their data using the Optical Size Estimation Model (OSEM), based on a Lambertian spherical phase function correction to zero degree phase angle and an albedo of 0.1. Just as with the SEM, the OSEM is used to statistically relate optical brightness to physical size. Caution is urged when attempting to use this model to determine the size of an individual object.

2. PHASE FUNCTIONS

To understand the assumptions behind this model, it is important to describe the concepts being used. The phase angle is defined as the angle between the Sun and the observer, as measured at the RSO (Fig. 1). There are two simple approximations for optical reflection properties: specular and diffuse. Specular reflections are those we normally associate with a highly polished surface, such as a mirror. Most objects are not mirror-like, but have some degree of surface roughness. Hence, the observed reflections are a composite of those from numerous small surfaces oriented at varying angles to our line of sight. This is characterized by an optical reflectance distribution known as the Lambertian distribution. In general, surface reflectance can be much complex than a linear combination of specular and Lambertian features, although this combination can often be a good approximation.

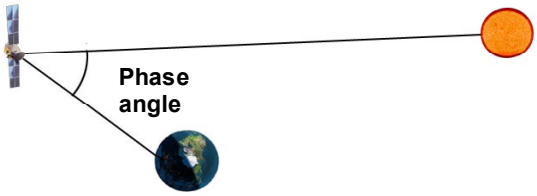

Figure 1. Phase angle.

The optical brightness of an RSO is measured in visual magnitudes. A difference in 5 magnitudes corresponds to a factor of 100 in intensity. The magnitude scale is inverted, so that a 1st magnitude object is brighter than a 2nd magnitude object. In the following plots, the magnitude has been normalized for range (40,000 km for GEO objects). Plotting the magnitude of the object versus the phase angle is known as the phase function. Fig. 2 illustrates three commonly used phase functions: 1) the lunar phase function, 2) the specular sphere phase function, and 3) the Lambertian spherical phase function. Note that except for the specular sphere typical phase functions are monotonically decreasing in brightness as a function of phase angle. For scaling purposes, the lunar phase function has been adjusted to the same scale as the Lambertian and specular sphere phase functions. The relative size is shown on the right side of the plot. An increase of one magnitude in optical brightness corresponds to an increase in linear size of a factor of 1.58. It is interesting to note that a specular sphere and a Lambertian sphere with identical size and albedo have the same brightness at a phase angle of approximately 83 degrees. If we observe a Lambertian sphere at 90 degrees phase angle and then adjust the brightness for 0 degrees phase angle, the correction to its brightness is an increase of approximately 1 magnitude.

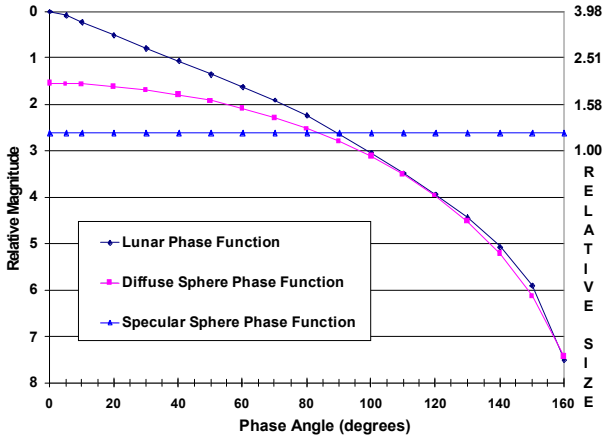

Figure 2. Three commonly used phase functions.

Barker et al developed the equations which define the size of the object in terms of the optically observed brightness. The observable parameter is the apparent brightness of target or the apparent magnitude, m_{app}, which is a function of band pass, time, distance, and phase angle. Almost all ground-based, photometric measurements are not spatially resolved, thus by definition the physical cross-section of a target must be defined by the solid angle subtended by the target and is measured in meters squared. The size or diameter referred to in this section is the diameter d of a disk or sphere seen at a distance R.

For solar illuminated objects the observed flux, F_{app}, is related to the solar flux F_{sun} in magnitudes and in a given pass band (such as V, R or I):

$$m_{app}(v) - M_{sun}(v) = -2.5 * \log\left[\frac{F_{app}(v)}{F_{sun}(v)}\right] \qquad (1)$$

Because the apparent brightness of an object varies as the square of the distance from the sun R_{sun}, and to the

object R, the apparent brightness is normalized to a standard distance Ro by the relation:

$$M_{abs}(v) = m_{app}(v) - 5.0 * \log\left[\frac{R}{R_o}\right] - 5.0 * \log\left[\frac{R_{sun}}{R_{sun(1AU)}}\right] \quad (2)$$

The observed flux F_{app}, reflected from an object with an optical cross section (OCS) is given by:

$$F_{app}(v) = OCS \cdot F_{sun}(v) = \Omega \cdot A_g \cdot \Psi(\alpha) \cdot F_{sun}(v) = \frac{\pi \cdot d^2}{4 \cdot R^2} \cdot A_g \cdot \Psi(\alpha) \cdot F_{sun}(v) \quad (3)$$

where Ω is the solid angle subtended by the object at a given distance or range R, or the physical cross section of the object with a diameter d. A is the Bond albedo which in turn is defined as the product of the geometrical albedo, A_g of the surface and the phase function, Ψ (α) which defines how the sunlight is scattered by the surface in a direction α to the observer. Rewriting, taking logs and solving for the diameter d:

$$d = \frac{2 \cdot R}{[\pi \cdot A_g \cdot \Psi(\alpha)]^{0.5}} \cdot 10^{\left[\frac{Mabs(v) - Msun(v)}{-5.0}\right]} \quad (4)$$

Eq. 4 is what we refer to as the OSEM correction with the geometric albedo equal to 0.1 and using the Lambertian phase function at 0 degrees phase angle.

3. SIMPLE SATELLITE SHAPES

In the 1960s, the US launched several spherical satellites for the purposes of radar and optical instrumental calibration. Two of these calibration spheres, SSN 1361 (Lincoln Calibration Sphere 1, 1965-034C) and SSN 1520 (Calsphere-4A, 1965-065H), can be used to demonstrate the utility and the limitations of the phase function approach. Fig. 3 illustrates the calibration sphere photometric signatures with respect to the Lambertian and specular phase functions. SSN 1520 clearly shows a phase function that tracks the shape expected for a diffuse sphere. SSN 1361 shows little or no systematic variation with phase angle, expected for a specular sphere. A detailed two-component albedo analysis of multiple observations, including the data shown in Fig. 3 (Hall et al., 2003. Lambert and Hall 2004), indicates that the reflectivity of SSN 1520 can be approximated very well by using a Lambertian albedo of ≈ 67% and a specular component of ≈ 1.2%, confirming the largely diffuse nature of this sphere. Similarly, the reflectivity of SSN 1361 is best modeled using Lambertian and specular albedos of ≈ 5.2% and ≈ 59%, respectively. This two-component albedo analysis cannot account for the small brightness variations seen in the signature of SSN 1361 (see Fig. 3), which are likely the result of small surface irregularities (Hall et. al., 2003, Lambert and Hall 2004). It does show that this aluminum sphere is basically a specular reflector. Deriving these albedo estimates for SSN 1361 and SSN 1520 requires knowledge of the diameter of each sphere. However, the goal of the OSEM is basically the reverse process: to provide rough size estimates using a purely Lambertian phase function with a nominal albedo of 10%. In the case of SSN 1520, this would cause OSEM to estimate a nominal diameter larger by a factor of ≈ 2.6 than the known diameter. For SSN 1361, a similar size inaccuracy would occur because of the nominal 10% OSEM albedo, and would be compounded by OSEM employing the inappropriate Lambertian phase function to adjust the measurements to zero phase-angle, which would ultimately yield nominal OSEM size-estimates that vary significantly with phase-angle even for this simple spherical satellite.

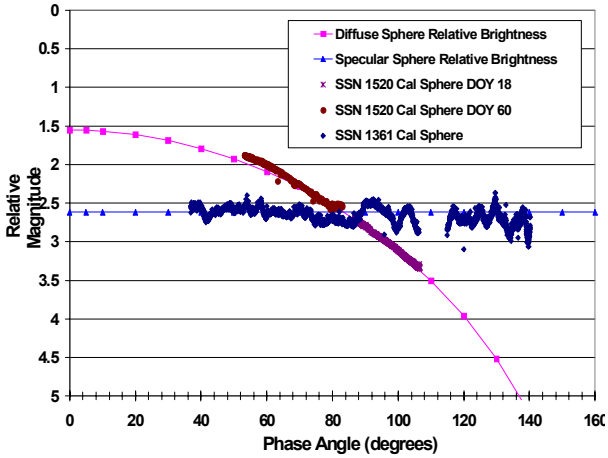

Figure 3. Phase functions for SSN 1361 and SSN 1520.

4. COMPLEX SATELLITE SHAPES

Because photometry is the measure of the brightness of a satellite at visible wavelengths, reflected sunlight dominates the observed satellite intensity. The photometric intensity will be strongly dependent on characteristics of the satellite being observed, such as shape, rotation, and surface properties. In general, the photometric brightness due to reflection from a surface is dependent on the characteristics of that surface, and the orientation of that surface with respect to both the Sun and to the location of the photometric detector. For unresolved objects, however, what is observed is the integrated brightness over all illuminated surfaces visible to the detector. Since most RSOs are not

spheres, their phase functions will not be represented by a specular or Lambertian sphere.

The range-normalized phase functions for four complex active GEO payloads are shown in Fig. 4. Note that these phase angle curves are quite different from the specular or Lambertian phase functions shown in Figs. 2 and 3. For three of the four payloads, the brightness decreases with phase angle, although not monotonically. However, for payload GSTAR 4, the brightness increases with phase angle, very different from the other three payloads, and from the spherical phase functions.

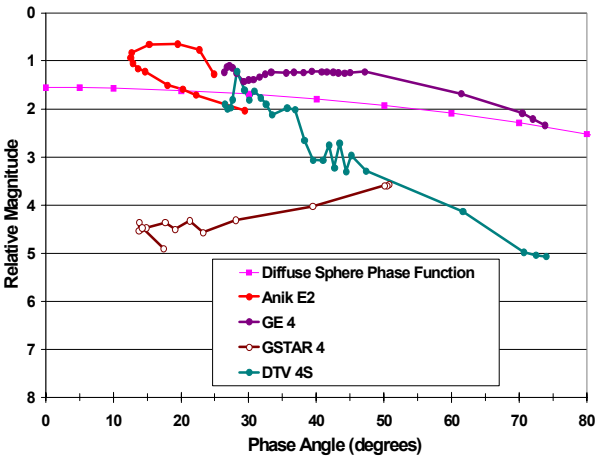

Figure 4. GEO payload phase angle curves.

We now apply the OSEM correction to the signatures for these satellites, which is shown in Fig. 5. It is clear that the resulting derived optical dimensions, shown on the right side of the plot, vary as a function of phase angle. In the case of payload DTV 4S, the size variation is greater than a factor of 4.

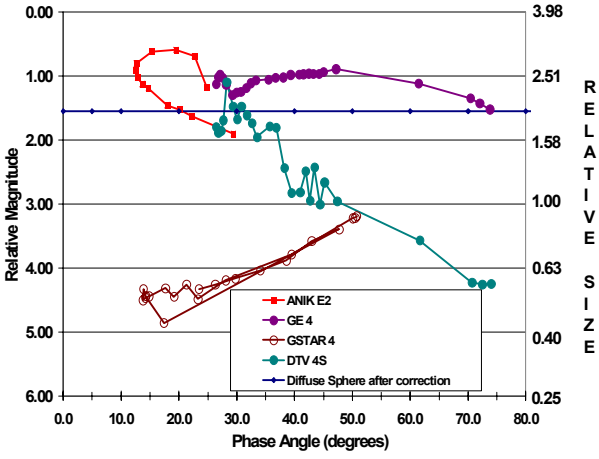

Figure 5. GEO payload size estimation using OSEM correction.

The loop in the ANIK E2 phase curve shown in Fig. 5 is a well-known phenomena for GEO satellites. It is due to the nature of the difference in the optical properties between the leading (east) and trailing (west) surfaces of the satellite. The change in slope happens at satellite local midnight, when the solar illumination changes from the trailing surfaces to the leading surfaces. This is illustrated in Fig. 6. The brightness at a given phase angle can vary dramatically, depending on the differences (shape, composition, shadowing) between the leading and trailing surfaces, and when the satellite is observed. These differences would result in different size estimations.

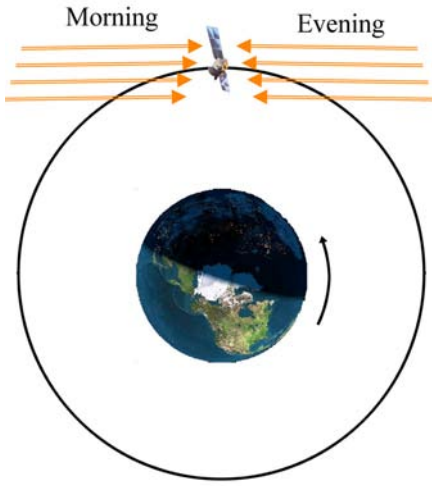

Figure 6. Daily illumination variation.

5. GEO DEBRIS OBJECTS

GEO debris objects may have even more interesting signatures as a function of phase angle. Fig. 7 illustrates the observations for four different debris objects. Note the large variation in the brightness of SSN 11581 in particular. It varies by more than four magnitudes at almost the same phase angle. This variation results in linear dimension changes of more than a factor of six.

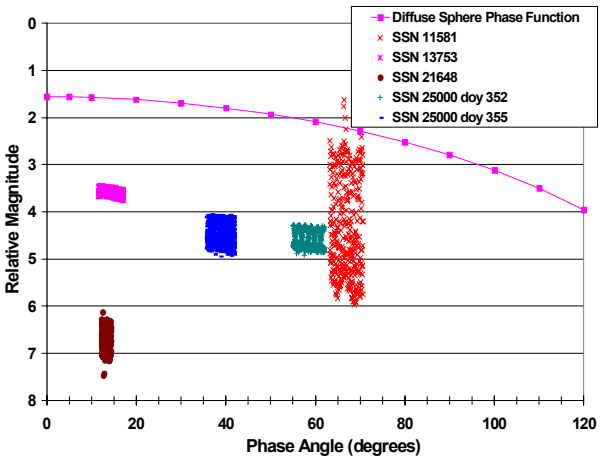

Figure 7. GEO debris phase angle curves.

Fig. 8 illustrates a single, 20 second exposure from a Raven telescope (Nishimoto et al., 1999) during an IADC debris campaign. This data was taken with the Raven telescope in GEO-tracking mode, so that the GEO object appears as a dot, while the stars streak through the field. The satellite brightness is obtained by comparing its brightness to the brightness of the background stars. Because the observations are obtained in unfiltered (white) light, the overall accuracy in the size estimation for this single exposure is about 30% (Barker et al, 2004). There is no indication of any brightness variability in this single, 20 second exposure image.

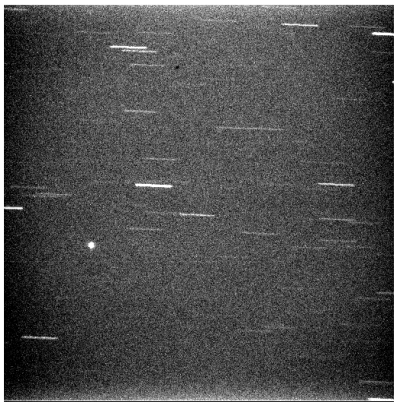

Figure 8. Tracking at GEO rates.

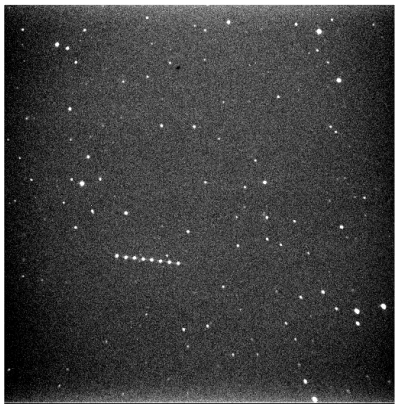

Figure 9. Tracking at sidereal rate.

Fig. 9 shows the same object with the telescope tracking at sidereal rate. In this case the stars appear as points while the satellite streaks through the field. This telescope tracking technique allows changes in satellite brightness to be observed as each pixel in the image provides an effective exposure time of about 250 msec. The variation in brightness for this satellite is easily seen in this figure. Depending upon the integration time used and the actual variation period, the size determination from the brightness would be quite variable.

Fig. 10 presents the observed phase angle function for a GEO satellite for various solar declinations. The red triangles represent observations obtained in the winter, when the Sun is below the celestial equator. The yellow squares represent observations obtained in the spring and fall, when the Sun is nearly in the plane of the celestial equator. The green circles represent observations obtained in the summer, when the Sun is above the celestial equator. This effect, which is due to the changing position of the Sun with respect to the Earth during different seasons, is illustrated in Fig. 11. It can be seen that this satellite's brightness is a function of top (north) and bottom (south) illumination. Again, correcting the object's brightness as if it were a Lambertian sphere can lead to quite variable sizes.

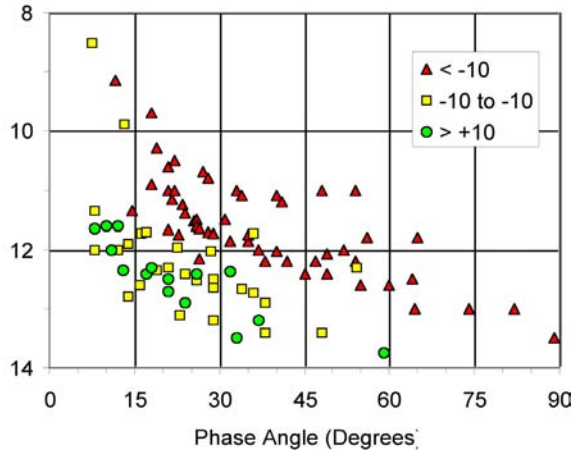

Figure 10. Solar declination variation.

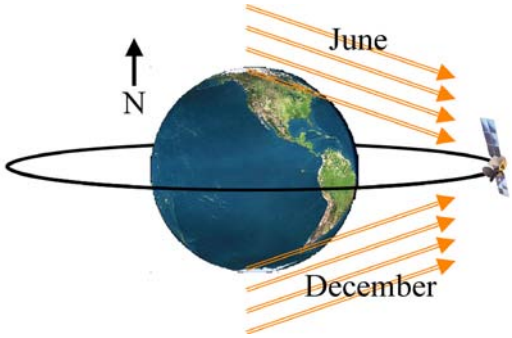

Figure 11. Seasonal illumination variation.

6. CONCLUSION

Although the OSEM provides a method of converting satellite optical brightness to physical size, there can be dramatic variations in the computed size of a single satellite, depending on satellite shape, as well as observing and illuminating conditions. Even if there is little variation in brightness, the calculated size may be incorrect, due to albedo effects or to insufficient sampling of the light curve. One must use caution in interpreting the OSEM data, keeping in mind the assumptions that are made in the model. One cannot

accurately determine the size of an object without sufficient information on all conditions and assumptions.

7. REFERENCES

Barker E., et al. Analysis of Working Assumptions in the Determination of Populations and Size Distributions of Orbital Debris from Optical Measurements, *Proceedings of the 2004 AMOS Technical Conference*, Wailea, Maui, HI, 2004.

Bohannon G. E. and Young N., *Debris Size Estimation Using Average RCS Measurements,* XonTech, Inc Report 930781 BE 2247, 1993.

Hall D., et al. AEOS I-Band Photometry of Moving Targets, *Proceedings of the 2003 AMOS Technical Conference*, Kihei, Maui, HI, 2003.

Lambert J. and Hall D., Non-Imaging SOI Calibration Sphere Surface Feature Resolution, *Non-Resolvable Space Object Identification Workshop,* Kihei, Maui, HI, 2004.

Nishimoto D., Kervin P., Africano J., Sydney P., and Soo Hoo V., Raven: The Evolution of Small Telescopes, *Proceedings of the 1999 AMOS Technical Conference*, Kihei, Maui, HI, 1999.